

Influence of Li conditioning on Lower Hybrid Current Drive efficiency in H-mode and L- mode plasmas on EAST

Marc Goniche^{a,*}, Miaohui Li^b, Yves Peysson^a, Yingjie Chen^b, Bojiang Ding^b, Annika Ekedahl^a, Haiqing Liu^b, Yong Liu^b, Jinping Qian^b, Xiuda Yang^b, Qing Zang^b, Tao Zhang^b, Sun Zhen^b, Xiao-Lan Zou^a and the EAST Team

^aCEA, IRFM, F-13108 Saint Paul-lez-Durance, France

^bInstitute of Plasma Physics, Chinese Academy of Sciences, Hefei 230031, People's Republic of China

Abstract. The lower hybrid current drive efficiency on the EAST tokamak is estimated on a large database of low loop voltage discharges ($V_L < 120\text{mV}$) covering the 2016 campaign starting with lithium-free plasma facing components and ending with strong cumulated deposition of lithium. The efficiency is found to vary in a wide range from 0.6 to $1.2 \times 10^{19} \text{A.W}^{-1} \text{m}^{-2}$. No deleterious effect of the density on the efficiency is found between 2.3 and $3.2 \times 10^{19} \text{m}^{-3}$. The high efficiency occurs after strong lithium evaporation. The low effective charge Z_{eff} and the higher temperature $\langle T_e \rangle$ of these discharges, can account for the high efficiency according to the expected scaling with Z_{eff} and $\langle T_e \rangle$. Modelling with a ray-tracing code coupled to a Fokker-Planck solver supports this result, assuming that the fast electron transport is reduced in the zero loop voltage discharge with high efficiency.

1. Introduction

Lower Hybrid waves are recognized to be an efficient tool to drive current with high efficiency. Fully or partially ($V_{\text{loop}} < 0.1\text{V}$) non-inductive long discharges have been obtained with lower hybrid current drive (LHCD) on several superconducting tokamaks: Tore Supra [1,2,3], TRIAM [4], EAST [5]. A one-minute H-mode discharge has been recently obtained on EAST [6]. This discharge, achieved with LHCD combined with other heating methods (ICRH, ECRH and NBI), has low and steady plasma radiation thanks to the lithium coating of the plasma facing components (PFC) and in particular of the divertor tungsten tiles. Lithium coverage reduces the effective charge Z_{eff} of the plasma by trapping the oxygen atoms [7,8]. It also reduces the particle recycling leading to a change of the n_e and T_e profiles at the plasma edge, including the scrape-off layer [4]. Both effects can be beneficial to the penetration of the wave and the current drive efficiency $\eta = nR_{\text{LH}}/P_{\text{LH}}$.

2. The experimental database

LHCD efficiency was estimated from a data base covering 160 L-mode and H-mode discharges with low loop voltage ($-0.02\text{V} < V_L < 0.12\text{V}$), a line-averaged density ($\langle n_e \rangle_{\text{lin}}$ in the $2.0\text{-}3.5 \times 10^{19} \text{m}^{-3}$ range. The plasma is in the upper single-null (USN) configuration with a current I_p in the $0.4\text{-}0.5\text{MA}$ range and a toroidal field of 2.25T or 2.45T . The database, covering the 2016 experimental campaign from March to October, includes discharges with lithium-free plasma facing components (5-10 March), discharges with lithium dropping during the plasma ramp-up phase (10 March) and discharges with lithium coating before the experimental day (11 March – 11 October). Data are averaged on a time slice of 3 seconds

(respectively from 1 to 3 s) for 83% (respectively 100%) of the discharges.

LHCD is provided by the 2.45GHz ($0\text{-}1.5\text{MW}$) and 4.6GHz ($1\text{-}2.7\text{MW}$) multijunction antennas [9]. The 2.45GHz (resp. 4.6GHz) antenna is an array of 5 (resp. 12) rows of 32 (resp. 48) narrow waveguides. In addition, ICRH ($0\text{-}0.8\text{MW}$), ECRH ($0\text{-}0.5\text{MW}$) and NBI ($0\text{-}2.7\text{MW}$) provide plasma heating. Total power is in the $2\text{-}5\text{MW}$ range. The parallel wave index N_{\parallel} of the 2.45GHz (resp. 4.6GHz) antenna can be varied between 1.85 and 2.6 (resp. 1.6 and 2.25), but most of the discharges were performed with $N_{\parallel} = 1.8$ or 2.1 on both antennas.

The mean power reflection coefficient RC is in the $2\text{-}7\%$ (resp. $1\text{-}6\%$) range for the 2.45GHz (resp. 4.6GHz) antenna. This range is consistent with the RF modelling, provided by the ALOHA code [10], indicating an equivalent range of electron density in front of the launcher of $2\text{-}10$ (resp. $1.3\text{-}5$) time the cut-off density at 2.45GHz (resp. 4.6GHz).

The current drive efficiency for low loop voltage (V_L) discharges can be estimated by plotting V_L as a function of the normalized LHCD power $P_{\text{norm}} = P_{\text{LH}} / (\langle n_e \rangle R_{\text{ip}})$. Keeping the first-order term of the dielectric tensor, namely the hot conductivity σ_{hot} , the relative loop voltage drop $\Delta V_L / V_L = (V_0 - V_L) / V_L$ with respect of the ohmic heating loop voltage V_0 can be expressed as

$$\rho \left[\left(-\frac{\Delta V_L}{V_L} \right) - \left(1 - \frac{1}{\rho} \right) \right] = \frac{(\eta + \eta_h) P_{\text{norm}}}{1 + \eta_h P_{\text{norm}}} \quad (1)$$

With the following notations: $\rho = (R_{\text{sp}})_{\text{LH}} / (R_{\text{sp}})_{\text{OH}} = (Z_{\text{LH}} / Z_{\text{OH}}) (T_{e,\text{LH}} / T_{e,\text{OH}})^{-3/2}$, $(R_{\text{sp}})_{\text{LH}}$ and $(R_{\text{sp}})_{\text{OH}}$ are the plasma resistivity in the LHCD and ohmic phase, respectively, η is the LHCD efficiency, $\eta_h = \sigma_{\text{hot}} / (P_{\text{norm}} \sigma_{\text{sp}})$, σ_{sp} being the Spitzer conductivity. For low loop voltage discharges $dP_{\text{norm}} = 1/\eta - P_{\text{norm}} \ll 1$ and equation (1) can be linearized as follows

*Corresponding author: marc.goniche@cea.fr

$$V_L = \frac{V_0}{\rho} \frac{\eta}{1 + \eta_h/\eta} \left(\frac{1}{\eta} - P_{\text{norm}} \right) \quad (2)$$

We therefore expect the slope of the curve V_L vs P_{norm} to be weakly varying as long as P_{norm} does not vary too much ($P_{\text{norm}}=0.8-1.3$ for these discharges). This quasi-linear relationship, verified on Tore Supra [2], allows an estimate of the efficiency with an accuracy of $\pm 10\%$ for $V_L < 100\text{mV}$. This efficiency includes the bootstrap current in the total non-inductive current but in these low beta discharges, the fraction of bootstrap current does not exceed 10-15% of the plasma current.

On EAST, the loop voltage with 1MW launched by the 2.45GHz antenna ($V_L=0.27\text{V}$) is much higher than that with the same power launched by the 4.6GHz antenna ($V_L=0.15\text{V}$) suggesting a lower efficiency for the 2.45GHz antenna [9, 11]. On a large database where the two current drive systems were combined, the loop voltage data (but also the stored energy data) are found to be more consistent assuming the efficiency of the 2.45GHz antenna is half of that of the 4.6GHz. Even with a matched wave index the power spectra $P(N_{||})$ are slightly different and the efficiency, estimated from a $1/N_{||}^2$ -weighted directivity, indicates a higher value by $\sim 20\%$ for the 4.6GHz antenna. However, modelling with a ray-tracing code coupled to a Fokker-Planck solver (C3PO/LUKE) [12] does not indicate a higher LHCD efficiency of the 4.6GHz antenna. Parasitic interaction of the wave with the plasma edge such as wave scattering or parametric decay has been evoked as a possible explanation of this reduced efficiency [9,11]. We therefore weighted the power launched by the 2.45GHz ($P_{2.45}$) antenna by a factor 0.5 to obtain a ‘4.6GHz-equivalent’ efficiency. In this database, the ratio $P_{2.45}/P_{4.6}$ does not exceed 0.5 in most cases and this correction affects the efficiency by no more than $\sim 20\%$.

For the range of magnetic field and plasma density of these discharges, the accessibility of the wave to the plasma core is restricted to the outer half plasma. The Stix-Golant condition $N_{||} > [1 - \omega_{pi}/\omega)^2 + (\omega_{pe}/\omega_{ce})^2]^{1/2} + \omega_{pe}/\omega_{ce}$, where ω , ω_{pi} , ω_{pe} , ω_{ce} are respectively the wave, ion plasma, electron plasma and electron cyclotron frequency, indicates a penetration of the wave up to a normalized radius $r/a \sim 0.8$ ($B_t=2.25\text{T}$) - ~ 0.7 ($B_t=2.45\text{T}$) for a line-average density $\langle n_e \rangle_{\text{lin}} = 3 \times 10^{19} \text{m}^{-3}$ and $N_{||}=2$. It should be kept in mind that this condition is an approximation which holds for cold plasma with no toroidal effect and further details on power absorption from C3PO/LUKE modelling will be given in section 4.

3. Experimental LHCD efficiency

Figure 1 shows the loop voltage as a function of the normalized power P_{norm} for the $B_t/I_p=2.25\text{T}/0.4\text{MA}$

case. Most of the points lie between $\eta=0.7 \times 10^{19} \text{A.W}^{-1} \text{m}^{-2}$ and $\eta=0.85 \times 10^{19} \text{A.W}^{-1} \text{m}^{-2}$ (broken lines) with no ordering of the efficiency with the density indicated by the colour code.

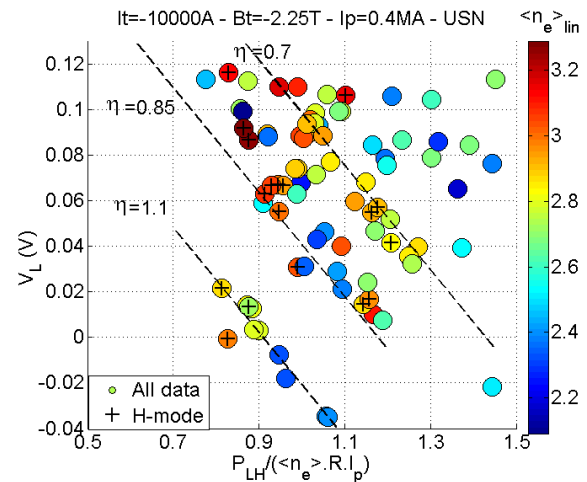


Fig. 1. Loop voltage V_L as a function of normalized power P_{norm} ($B_t/I_p=2.25\text{T}/0.4\text{MA}$, USN).

However, there are a significant number of discharges which have a higher efficiency ($\eta \sim 1.1 \times 10^{19} \text{A.W}^{-1} \text{m}^{-2}$). When the extrapolated efficiency is plotted as a function of the discharge number, these high efficiency discharges are all obtained late in the campaign when the cumulated amount of the lithium evaporated exceeds 150-200g (Figure 2). Lithium aerosols during the discharge, between the two broken lines of figure 2, do not seem to improve the efficiency. Most of the H-mode discharges have a high efficiency, between 0.8 and $1.15 \times 10^{19} \text{A.W}^{-1} \text{m}^{-2}$.

Late in the campaign, the plasma current was raised to 0.5MA ($B_t=2.45\text{T}$). The efficiency is in the $0.85-1.1 \times 10^{19} \text{A.W}^{-1} \text{m}^{-2}$ range and, on a statistical basis, no improvement with respect of the 2.25T/0.4MA case (same period of the campaign) is observed. On other tokamaks, a beneficial effect of I_p (scaling as $I_p^{1/2}$) [13,14] has been inferred and a slight increase of $\sim 12\%$ could be expected when the current is increased from 0.4MA to 0.5MA. The internal inductance l_i , from the equilibrium code EFIT, decreases with plasma density from 1.2 ± 0.1 ($\langle n_e \rangle_{\text{lin}} = 2.3 \times 10^{19} \text{m}^{-3}$) to 0.95 ± 0.1 ($\langle n_e \rangle_{\text{lin}} = 3.0 \times 10^{19} \text{m}^{-3}$) with no significant effect of the LH power.

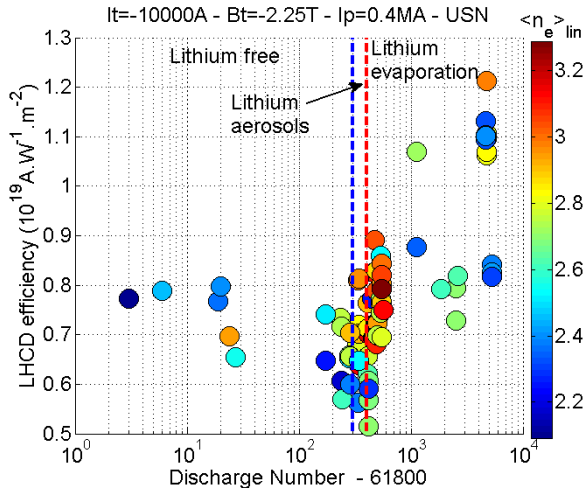


Fig. 2. Time history of the LHCD efficiency ($B_t/I_p=2.25\text{T}/0.4\text{MA}$, USN).

In addition to the effect of lithium coverage of the PFCs, the efficiency is closely related to the LH coupled power (figure 3-a) and η values above 1 are only obtained at moderate power launched by the 4.6GHz, between 1.4 and 1.8MW. Moreover these high efficiency discharges have all radiation from the bulk plasma, between 0.3 and 0.5MW.

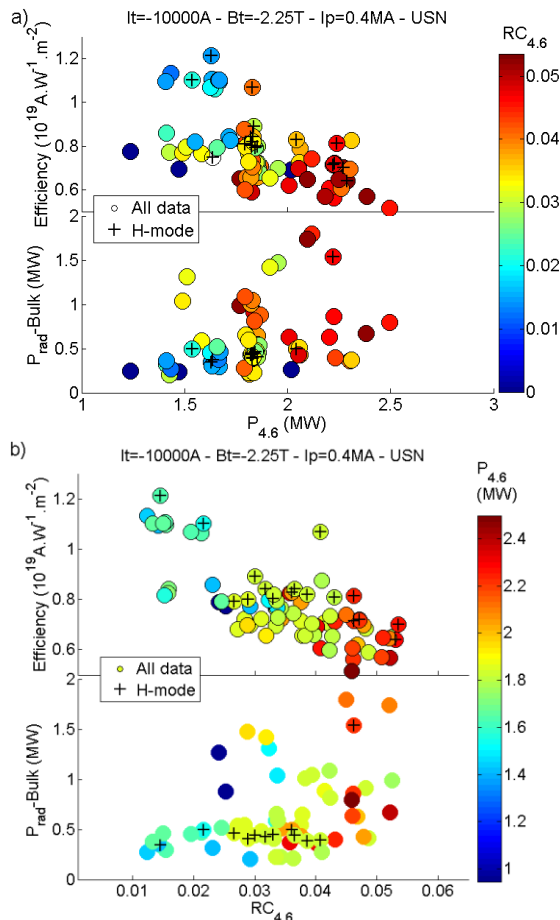


Fig.3. LHCD efficiency and radiated power in the main plasma as a function of a) power b) reflection coefficient of the 4.6GHz antenna.

The correlation between the efficiency and the power reflection coefficient of the 4.6GHz launcher $RC_{4.6}$ is even better (figure 3-b). The increase of the RC with the launched power indicates non-linear interaction of the RF electric field with the plasma facing the antenna, namely ponderomotive forces as observed and modelled on Tore Supra [15]. Although a change of RC from 1-2% to 4-5% cannot explain a modification of the wave spectrum such as the CD efficiency is reduced by a factor 2, it suggests that the spectrum could be further modified when the RF electric is high due to wave scattering or parametric decay [9, 11].

4. LHCD Modelling

From this database, 5 discharges with same line-average density ($\langle n_e \rangle_{\text{lin}}=2.95 \times 10^{19} \text{m}^{-3}$), plasma current ($I_p=0.4\text{MA}$) and magnetic field ($B_t=2.25\text{T}$) were selected: 61824 (before any lithium evaporation), 62209-62296-62349 (after weak lithium evaporation, 12-25-37g) and 66526 (after strong lithium evaporation, >150g). The 3 weak lithium evaporation discharges were performed with different values of N_{\parallel} (1.82-2.04-1.60). The density profiles, from the Thomson scattering system, were re-scaled to match the line-average density provided by the far infra-red interferometer (with a scaling factor varying between 0.7 and 1.0). The temperature profiles are also provided by the Thomson scattering diagnostic. These profiles, along a vertical chord, were mapped to the mid-plane using the EFIT equilibrium code (figure 4). For these discharges the profiles are very similar except #66526 (high lithium case) which has a less peaked density and a more peaked temperature. The total LH power varies between 1.9MW and 2.5MW, the mean effective charge Z_{eff} between 2.7 and 4.9 according to the bremsstrahlung diagnostic ($Z_{\text{eff}}\text{-Brem}$). Z_{eff} was also estimated from the radiated power with the Matthews' law ($Z_{\text{eff}}\text{-Mat}$) [16] (Table1).

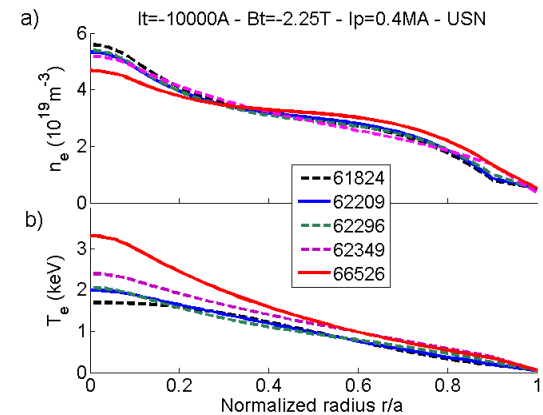


Fig. 4. a) density b) electron temperature profiles. The 5 pulses have the same line-average density ($\langle n_e \rangle_{\text{lin}}=3.0 \times 10^{19} \text{m}^{-3}$).

The loop voltage varies between 59mV and 88mV for the no or weak lithium cases and is -1mV for the strong lithium case. The resulting efficiency is found to be between 0.70 and $0.80 \times 10^{19} \text{A.W}^{-1} \cdot \text{m}^{-2}$ for the no or weak lithium cases but jumps to $1.2 \times 10^{19} \text{A.W}^{-1} \cdot \text{m}^{-2}$ for the strong lithium case. Following the temperature scaling ($\sim T_e^{0.5}$) found on Tore Supra [13] and FTU [14] and the Z_{eff}

($\sim (5+Z_{\text{eff}})^{-1}$) scaling from the 1-D Fisch's theory[17], the efficiency normalized to the volume-averaged temperature $\langle T_e \rangle = 1 \text{keV}$ and $Z_{\text{eff}} = 2$ lies between 0.96 and 1.25 except for the no lithium case for which the Z_{eff} could be over-estimated and the low N_{\parallel} discharge for which the wave accessibility is poor.

Pulse #	Li (g)	P_{LH} (MW)	N_{\parallel} 4.6GHz	V_1 (mV)	Z_{eff} Brem	Z_{eff} Mat	η ($10^{19} \text{A.W}^{-1} \cdot \text{m}^{-2}$)	Norm. η ($10^{19} \text{A.W}^{-1} \cdot \text{m}^{-2}$)
61824	0	2.37	1.82	88	4.9	5.0	0.76	1.36
62209	12.5	2.03	1.82	89	2.7	2.6	0.72	0.96
62296	25	2.52	2.04	59	2.7	2.4	0.80	1.03
62349	37.5	2.16	1.60	66	3.5	2.2	0.70	0.78
66526	>150	1.88	2.04	-1	4.1	1.9	1.21	1.25

Table 1. Main parameters of the modelled discharges with same density ($\langle n_e \rangle_{\text{lin}} = 2.95 \times 10^{19} \text{m}^{-3}$).

In order to validate further the effect of lithium, the C3PO/LUKE code was run for these 5 discharges. Most of the power is absorbed at $r/a=0.5-0.7$ with, for some of them, a significant part of the power absorbed in the very core ($r/a < 0.3$). It was found that for the 4 no/weak lithium discharges, with residual loop voltage, the efficiency is correctly modelled when a diffusion coefficient of the fast electrons is included in the model. For the strong lithium discharge, the modelled and experimental efficiencies match when no transport for the fast electrons is assumed (Figure 5-a). This could be the result of an internal transport barrier for this fully non-inductive discharge which has a much higher central electron temperature. The modelled internal inductance is also consistent with the values obtained from the EFIT equilibrium code within 10-15% in most cases (Figure 5-b).

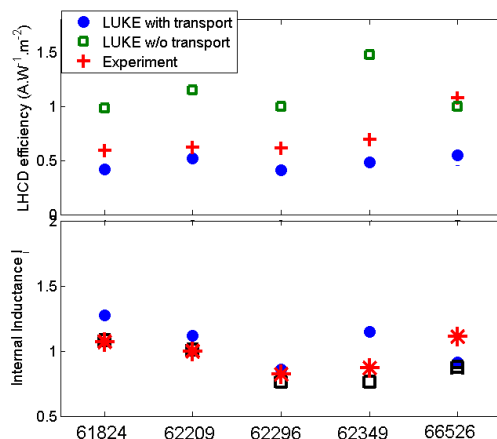


Fig. 5 a) Efficiency b) Internal inductance from experiment and modelling for the 5 discharges of the table 1.

5. Conclusions

The analysis of LHCD efficiency for discharges with more than 70% of the current is driven by the 4.6GHz antenna shows a beneficial effect of wall coverage with lithium. This was also observed with the 2.45GHz antenna [18]. This effect is partly due to the lower radiation and consequently lower Z_{eff} and higher temperature of the plasma. However, the normalized efficiency of the discharge performed after strong lithium evaporation indicates a higher efficiency by about 25% and edge plasma-wave interaction affecting the wave spectrum cannot be ruled out. This assumption is also supported by the correlation between the efficiency and the RF electric field which is a function of launched power and reflection coefficient. However, no deleterious effect of the density between 2.3 and $3.2 \times 10^{19} \text{m}^{-3}$ on the efficiency is found from this large database.

The CEA/IRFM members warmly acknowledge the hospitality of the ASIPP Team during the visits to EAST. This work is supported by the National Magnetic Confinement Fusion Program of China (Grant No 2015GB10200) and the Associated Laboratory CEA/IRFM – CAS/ASIPP. This work has been carried out within the framework of the EUROfusion Consortium and has received funding from the European research and training programme under grant agreement N° 633053. The views and opinions expressed herein do not necessarily reflect those of the European Commission.

References

- [1] D.Van Houtte et al. Nucl. Fusion **44** (2004) L11–L15
- [2] M.Goniche et al., Physics of Plasmas **21** 061515 (2014)
- [3] R.J.Dumont et al., Plasma Phys. Control. Fusion **56** (2014) 075020 (11pp)
- [4] H.Zushi et al., Nuclear Fusion **45** (2005) S142–S156.

- [5] H.Y.Guo et al., Phys. Plasmas 19, 056124 (2012)
- [6] B.N.Wan et al., 26th IAEA FEC, Kyoto, 17-22 October 2016
- [7] G.S.Xu, Nucl. Fusion 51 (2011) 072001 (6pp)
- [8] L.Chen et al., Nucl. Fusion 56 (2016) 056013
- [9] M. H.Li et al. Phys. Plasmas 23, 102512 (2016)
- [10] J.Hillairet et al., Nucl. Fusion 50, 125010 (2010)
- [11] B.J.Ding et al., 26th IAEA FEC, Kyoto, 17-22 October 2016
- [12] Y.Peysson, Y. and J.Decker, FST, 65 (2014) 22
- [13] M.Goniche et al., 16th Topical Conference on Radio Frequency Power in Plasmas (2005), AIP Conf. Proc. 787, pp. 307-310; doi: <http://dx.doi.org/10.1063/1.2098245>
- [14] V.Pericoli Ridolfini et al., Nucl. Fusion 45 (2005) 1386–1395
- [15] M.Preynas et al., Nucl. Fusion 53 (2013) 013012,
- [16] G.F.Matthews et al., J. Nucl. Mat. 241-243 (1997) 450-455
- [17] N.J.Fisch 1987 Rev. Mod. Phys. **59** 175–234
- [18] B.J.Ding et al., Nucl. Fusion 55 (2015) 093030